



**HAL**  
open science

## Comparison of the temperature and field dependencies of the critical current densities of bulk YBCO, MgB<sub>2</sub> and iron-based superconductors

Anjela Koblichka-Veneva, Michael Rudolf Koblichka, Kévin Berger, Quentin Nouailhetas, Bruno Douine, Muralidhar Miryala, Masato Murakami

### ► To cite this version:

Anjela Koblichka-Veneva, Michael Rudolf Koblichka, Kévin Berger, Quentin Nouailhetas, Bruno Douine, et al.. Comparison of the temperature and field dependencies of the critical current densities of bulk YBCO, MgB<sub>2</sub> and iron-based superconductors. *IEEE Transactions on Applied Superconductivity*, 2019, 29 (5), pp.1-5. 10.1109/TASC.2019.2900932 . hal-01988008v2

**HAL Id: hal-01988008**

**<https://hal.science/hal-01988008v2>**

Submitted on 15 Feb 2019

**HAL** is a multi-disciplinary open access archive for the deposit and dissemination of scientific research documents, whether they are published or not. The documents may come from teaching and research institutions in France or abroad, or from public or private research centers.

L'archive ouverte pluridisciplinaire **HAL**, est destinée au dépôt et à la diffusion de documents scientifiques de niveau recherche, publiés ou non, émanant des établissements d'enseignement et de recherche français ou étrangers, des laboratoires publics ou privés.

# Comparison of temperature and field dependencies of the critical current densities of bulk YBCO, MgB<sub>2</sub> and iron-based superconductors

A. Koblichka-Veneva, M. R. Koblichka, K. Berger, Q. Nouailhetas, B. Douine, M. Muralidhar and M. Murakami

**Abstract**—We compare the temperature and field dependence of the critical current densities of high- $T_c$  superconductor materials intended for various bulk applications like trapped-field magnets. This comprises bulk samples of YBa<sub>2</sub>Cu<sub>3</sub>O<sub>x</sub> (YBCO), MgB<sub>2</sub> and iron-based materials, including also various versions of the YBCO compound like melt-textured ones, infiltration-growth processed ones, and YBCO foams. Critical current densities and flux pinning forces were obtained from magnetization loops measured using Quantum Design SQUID and PPMS systems with applied magnetic fields of up to  $\pm 9$  T. The obtained data are compared to each other with respect of the optimal cooling temperature possible using modern cryocoolers. Furthermore, we plot the temperature dependencies of the critical current densities versus the normalized temperature  $t = T/T_c$ . This enables a direct judgement of the performance of the material in the trapped field applications.

**Index Terms**—YBCO, MgB<sub>2</sub>, iron-based superconductors, critical currents, temperature dependence.

## I. INTRODUCTION

THE magnetic properties of high- $T_c$  superconducting samples are commonly plotted like magnetization  $M$  or critical current  $j_c$  as function of applied field,  $H_a$ . However, if we want to compare different types of such superconductors with each other, the different values of the superconducting transition temperature,  $T_c$ , have to be considered as well as this defines which coolant or cooling procedure is required in an application. Therefore, the irreversibility lines,  $H_{irr}(T)$ , are often discussed in review articles [1], [2], when addressing the proper use of the superconducting materials.

For the application as superconducting permanent magnets, dubbed supermagnets or trapped field (TF) magnets, there are three different candidate materials available: (i) bulk, melt-textured single crystalline materials of YBa<sub>2</sub>Cu<sub>3</sub>O<sub>x</sub> (YBCO or RE-123, where RE indicates rare-earths) [3], [4], and a superconducting YBCO foam [5]. (ii) Bulk, polycrystalline MgB<sub>2</sub>

prepared in two different ways [6], [7] and (iii) bulk, polycrystalline iron-based superconductors (IBS) of Ba<sub>0.6</sub>K<sub>0.4</sub>Fe<sub>2</sub>As<sub>2</sub> (122) [8], [9] and FeSe with addition of Ag [10], [11] were chosen for comparison. The latter two types of material offer a much easier (and hence, cheaper) way of producing the samples as the grain boundaries (GBs) were found not to be weak-links, but do provide flux pinning like in the case of conventional superconductors like NbTi or Nb<sub>3</sub>Sn. For FeSe, which would be the simplest possible material free of toxic components, the GB pinning is still under question [12]–[14]. Furthermore, all these samples are free of rare earths.

To come to a decision which superconducting material offers the best-suited properties for applications regarding also the demands of the required cooling equipment, we investigated the temperature dependence of the critical current densities of several types of samples being interesting for the application as TF magnets. The sample preparation and the  $j_c(H)$  behavior of the selected samples are described in the references given. For most of the samples, new measurements were required using samples cut to smaller size (max.  $1 \times 1 \times 0.5$  mm<sup>3</sup>). For the RE-123 materials, we have chosen a bulk YBCO sample [15] prepared via the infiltration-growth (IG) process [16], [17], a strut of a YBCO foam due to its outstanding pinning properties [5], [18], [19], and a (Nd,Eu,Gd)-123 (NEG) melt-textured bulk with TiO<sub>2</sub>-nanoparticles enhancing the flux pinning properties [20], [21]. For MgB<sub>2</sub>, we selected a sample prepared via solid-state sintering [6], a spark-plasma sintered sample [7], [22] and a sintered sample with added carbon-encapsulated boron [23], [24]. Finally, for the IBS, we selected sintered FeSe with 4 wt.-% Ag [11], [25] and we took data of hot-isostatic processed (HIP) 122 sample from Weiss *et al.* [8], [9], where already data of TF measurements were published. For comparison, all  $j_c$  data are plotted versus the reduced temperature,  $t = T/T_c$ .

## II. EXPERIMENTAL PROCEDURE

Details of the sample preparation procedures of the samples investigated here can be found in the literature [5]–[8], [15], [20], [24]. Table I summarizes the superconducting transition temperatures,  $T_c$ , the transition width,  $\Delta T_c$ , and information about the measured sample size and the size available for TF experiments.

Magnetic measurements were performed using a Quantum Design MPMS3 SQUID system with  $\pm 7$  T applied field, and Quantum Design PPMS systems equipped either with an

Manuscript received xx.xx.xxxx. This work is a part of the SUPERFOAM international project funded by ANR and DFG under the references ANR-17-CE05-0030 and DFG-ANR Ko2323-10.

M. R. Koblichka and A. Koblichka-Veneva are with Experimental Physics, Saarland University, P.O. Box 151150, 66041 Saarbrücken, Germany. Present address: Department of Materials Science and Engineering, Shibaura Institute of Technology, 3-7-5 Toyosu, Koto-ku, Tokyo 135-8548, Japan.

K. Berger and B. Douine are with GREEN, Université de Lorraine, Vandoeuvre-lès-Nancy CEDEX, France.

Q. Nouailhetas is with GREEN, Université de Lorraine, Vandoeuvre-lès-Nancy CEDEX, France, and Saarland University, P. O. Box 151150, 66041 Saarbrücken, Germany.

M. Muralidhar and M. Murakami are with Department of Materials Science and Engineering, Shibaura Institute of Technology, 3-7-5 Toyosu, Koto-ku, Tokyo 135-8548, Japan.

extraction magnetometer or with VSM option ( $\pm 7$  T and  $\pm 9$  T applied magnetic field). In all cases, the field was applied perpendicular to the sample surface. The field sweep rate was always 0.36 T/min. From the magnetization data, the critical current densities,  $j_c$ , were evaluated using the extended Bean approach for rectangular samples [26]. The irreversibility lines were determined from the closing of the hysteresis loops from own measurements, except the literature data [8], where extrapolation from the  $j_c(H)$  graphs was employed [27].

### III. RESULTS AND DISCUSSION

The  $j_c(T)$ -data were extracted from the measured/published  $j_c(H_a)$ -data at 0.5 T, 1.0 T, 1.5 T, 2.0 T, 2.5 T, 3.0 T, 3.5 T, 4.0 T, 4.5 T and 5 T applied fields. These data are then plotted versus the reduced temperature,  $t = T/T_c$  to account for the differences in  $T_c$  between the samples of different origin or different treatments.

Figure 1 presents the temperature dependence of  $j_c$  for three different types of  $\text{MgB}_2$  samples. Data at temperatures below 10 K were severely influenced by flux jumps [28], which are a serious problem for bulk  $\text{MgB}_2$ . Therefore, the application temperature aimed for is commonly chosen to be 20 K ( $t \approx 0.52$ ), which is easily accessible using cryocoolers. The sintered, polycrystalline  $\text{MgB}_2$  sample treated at 775 °C shows only small current densities as compared to the sintered  $\text{MgB}_2$  sample where carbon-coated boron was added, and to the spark-plasma sintered  $\text{MgB}_2$  sample (HD1200), which shows a very high density (almost 99.2 % of the theoretical value). For the sintered, polycrystalline  $\text{MgB}_2$  samples, the reaction temperatures between 775 and 805 ° were found to be optimal in previous works [6], [29], [30], but a certain amount of porosity still remains in the samples which severely limits  $j_c$ . The sample HD1200 was spark-plasma sintered at 1200 °C, which may lead to the formation of some  $\text{MgB}_4$  particles, but these were found to be located mainly along the GBs and not within the  $\text{MgB}_2$  grains, where they would be more effective as flux pinning sites. The density of this sample reaches 99.2% of the theoretical value [7]. As a result, the  $\text{MgB}_2$  sample with 10 %-added carbon-coated boron exhibits the highest critical current densities of all  $\text{MgB}_2$  samples studied here. It is also important to point out that all  $\text{MgB}_2$  samples share the fact that only relatively small fields can be applied without severe reduction of  $j_c$ , so at 60% of  $T_c$ , only small currents can flow in the sample. This indicates that all  $\text{MgB}_2$  samples suffer from a relatively low  $H_{irr}(T)$  [1], [2], [31].

Figure 2 shows a similar comparison of three different types of REBCO samples, including an IG-processed, melt-textured bulk sample, a single strut of a superconducting YBCO foam and a NEG sample with addition of 0.1 mol-%  $\text{TiO}_2$  nanoparticles. The latter sample was found to exhibit very large critical current densities, especially at elevated temperatures [21]. The IG-processed YBCO sample and the YBCO foam strut share the preparation route using the IG-approach, but the foam strut stems from a real 3D structure, so the crystallographic texture is not in (001)-direction as in the case of the bulk piece. The microstructure of both types of samples is, however, similar to each other, and both

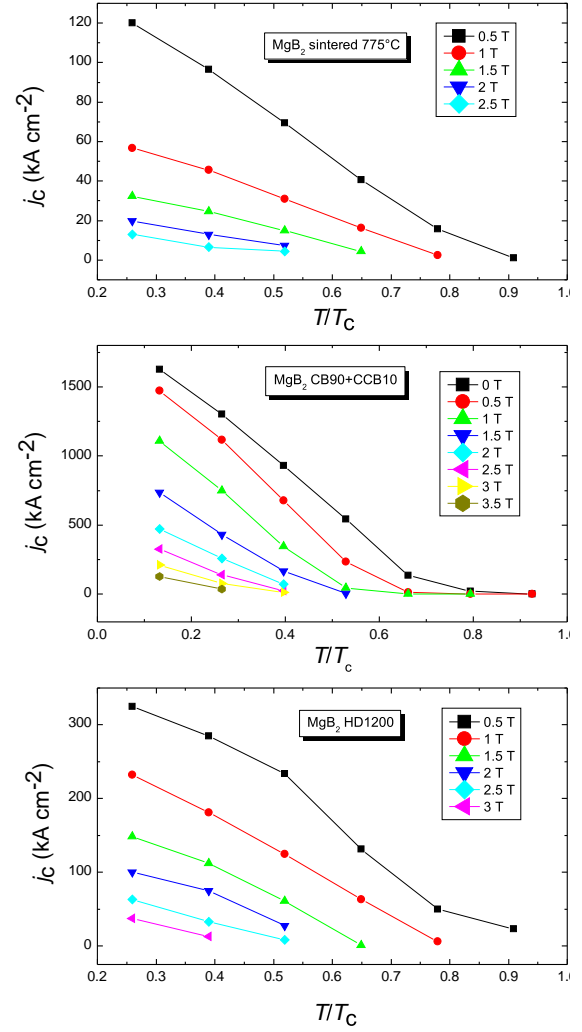


Fig. 1. Temperature dependence of  $j_c$  vs.  $t = T/T_c$  at various applied magnetic fields of selected  $\text{MgB}_2$  samples. The lines are guidelines for the eye.

samples share the presence of many, very small 211 particles as discussed in Ref. [18]. These particles provide additional flux pinning, and the pinning force scaling of these two sample types exhibit peak positions of  $\sim 0.5$  and a completely different shape of the resulting pinning function which resembles a dome-shape. The consequence is a clear upturn of  $j_c(T)$  at lower temperatures, and a slow increase between  $T_c$  and about  $t = 0.8$ . In the case of the NEG-sample doped with 0.1 mol-%  $\text{TiO}_2$  nanoparticles, these additional particles can provide additional flux pinning, which is mainly effective at elevated temperatures [21]. The resulting  $j_c(T)$ -curves show a much steeper upturn right away from  $T_c$ , yielding relative high  $j_c$  data at 77 K, and eventually, even applications at 90 K may become possible using such samples. The temperature aimed at for applications of the RE-123 samples is normally 77 K ( $t = 0.85$ ), which is very close to  $T_c$  as compared to the other materials. Cooling these samples to lower temperatures enables very large trapped fields to be realized, see e.g., the record trapped field values achieved in [3], [4].

Figure 3 presents finally the results of the two IBS samples.

TABLE I  
SUPERCONDUCTING PARAMETERS OF THE SAMPLES INVESTIGATED, DIMENSIONS, REFERENCES AND REMARKS.

Sample type	$T_c$ [K]	$\Delta T_c$ [K]	dimensions [mm <sup>3</sup> ]	Ref.	remarks
YBCO-IG	91	1.7	$1.5 \times 1.5 \times 0.5$	[15]	27 mm dia.
YBCO foam	91.1	3.2	$1.5 \times 0.7 \times 0.07$	[19]	single foam strut
NEG + 0.1 mol% TiO <sub>2</sub>	93.2	2.1	$1.5 \times 1.5 \times 0.5$	[20]	18 mm dia., 10 mm height
MgB <sub>2</sub> sintered	38.5	2.3	$1.5 \times 1.5 \times 0.5$	[6]	20 mm dia., 775°C reaction temp. electric and magnetic data available
MgB <sub>2</sub> HD1200	38.5	0.6	$1.5 \times 1.0 \times 0.5$	[7], [22]	spark-plasma sintered, 99.2% dense, up to 50 mm dia.
MgB <sub>2</sub> CB90+CCB10	37.8	1.8	$3.5 \times 3.0 \times 2.0$	[23], [24]	10% carbon-coated boron, 20 mm dia., 7 mm height
FeSe+4 wt.-% Ag polycryst.	9.42	0.98	$1.0 \times 1.0 \times 0.5$	[25]	10 mm dia, 7 mm height, electric and magnetic data available
Ba <sub>0.6</sub> K <sub>0.4</sub> Fe <sub>2</sub> As <sub>2</sub> (122)	37.1	7.5	no information	[8], [9]	HIP-processed, polycrystalline, 10 mm dia., 92% dense

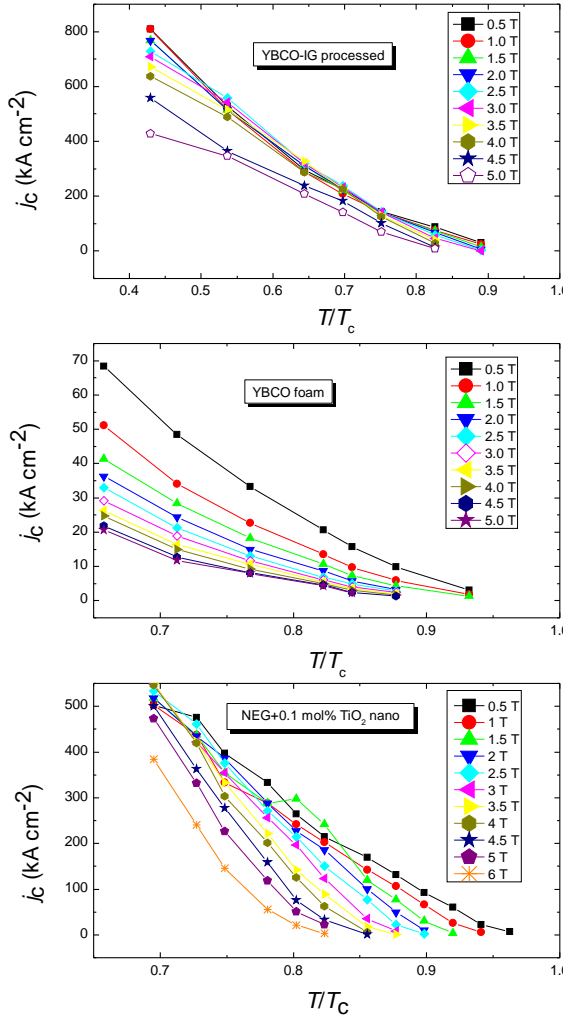


Fig. 2. Temperature dependence of  $j_c$  vs.  $t = T/T_c$  at various applied magnetic fields of selected REBCO samples. The lines are guidelines for the eye.

The first sample is a FeSe sample plus 4 wt.-% Ag [11], [25]. The Ag-addition proved to be effective to improve the superconducting properties of FeSe as well as the grain connectivity, allowing the use of the simple sintering process. The second type is a polycrystalline 122 sample, densified using

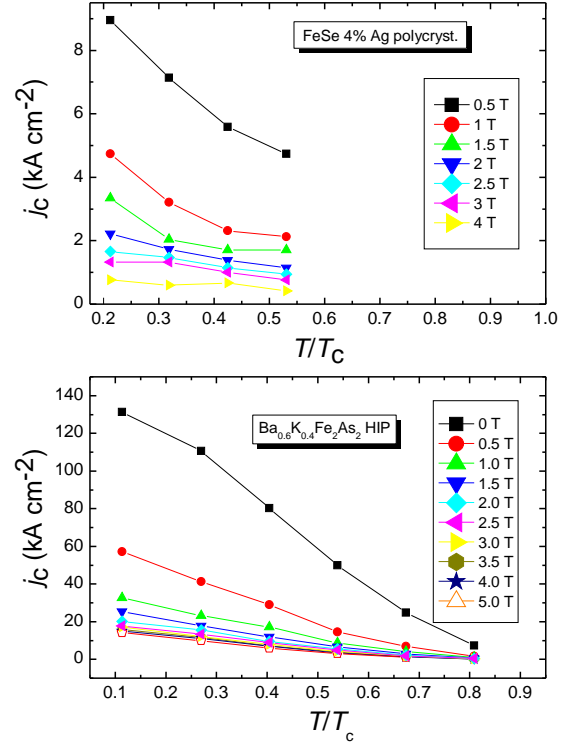


Fig. 3. Temperature dependence of  $j_c$  vs.  $t = T/T_c$  at various applied magnetic fields of the selected IBS samples (sintered FeSe + 4 wt.-% Ag and polycrystalline Ba<sub>0.6</sub>K<sub>0.4</sub>Fe<sub>2</sub>As<sub>2</sub> (122) after HIP). The lines are guidelines for the eye.

HIP [8], [9]. This type of sample was already demonstrated as TF magnet [9]. For IBS, the possible operation temperature would be 4.2 K ( $t \approx 0.47$  (FeSe) or  $t \approx 0.1$  for 122), which is for FeSe a similar reduced temperature like in the case of MgB<sub>2</sub>. The advantage of the IBS are the much larger magnetic fields possible, which is also seen from the higher  $H_{irr}(T)$  in Fig. 6 below. In Figs. 4 and 5, we finally compare the  $j_c(T)$  data at two selected applied fields, 0.5 T (Fig. 4) and 2 T (Fig. 5). At 0.5 T applied magnetic field, the superconducting properties of all samples are well developed. In contrast, 2 T is larger than the surface field of any permanent magnet, which makes this field a first target field for applications. Here, we can see that  $j_c(\text{REBCO}) > j_c(\text{MgB}_2) > j_c(\text{IBS})$ , with the

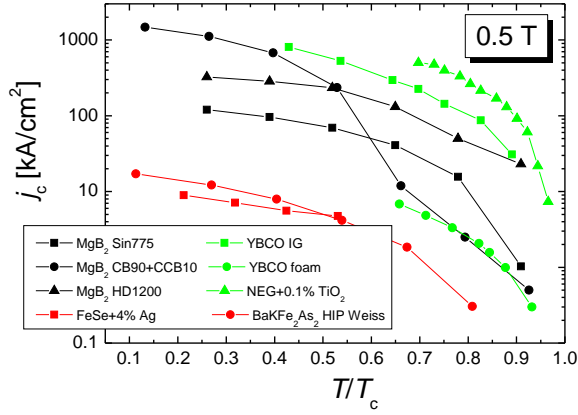


Fig. 4. Comparison of all samples at 0.5 T applied magnetic field.

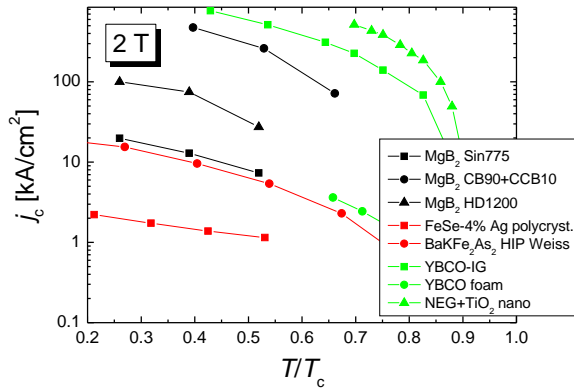


Fig. 5. Comparison of all samples at 2.0 T applied magnetic field.

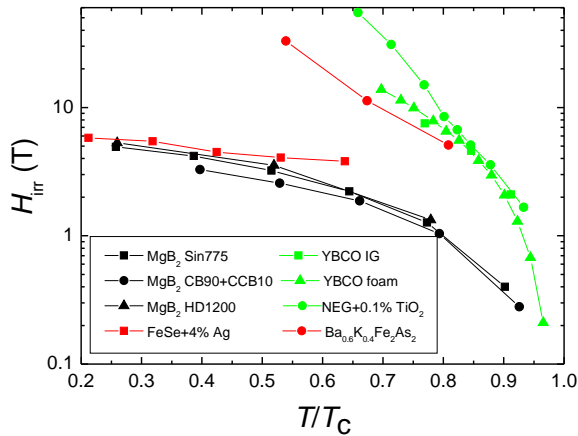


Fig. 6. Irreversibility fields of all samples plotted versus the reduced temperature,  $t = T/T_c$ .

exception of the lower  $j_c$  of the YBCO foams. Nevertheless, the large potential of the foams is demonstrated by the high irreversibility line (see below), so it could be possible to come close to  $j_c$  of the IG-processed bulks when the texture is further optimized [19]. The other REBCO materials develop high critical current densities already very close to their  $T_c$ , showing a steep increase when lowering  $T$ . All  $\text{MgB}_2$  samples exhibit a similar  $j_c(T)$  dependence, and the additional flux pinning sites get active only below  $t \approx 0.65$ . The  $j_c$  data of

the sample with added carbon are found to be comparable to those of YBCO, but for that the sample has to be cooled down to  $t \approx 0.4$ . At 20 K ( $t = 0.52$ ),  $j_c$  is still smaller as that of REBCO at 60 K ( $t = 0.66$ ).

Figure 6 presents  $H_{\text{irr}}(T)$  for all samples, plotted also versus the reduced temperature,  $t = T/T_c$ .  $H_{\text{irr}}(T)$ -data possible with the REBCO materials are fairly above the other two material systems. Also,  $H_{\text{irr}}(T)$  of the IG-processed materials is much higher than that of melt-processed samples, even with the addition of nanoparticles as flux pinning sites. This also applies for the IG-processed foam sample. All  $\text{MgB}_2$  samples reveal a very similar  $H_{\text{irr}}(T)$ -behavior, irrespective of the pinning sites added. The  $H_{\text{irr}}(T)$ -data of  $\text{MgB}_2$  and FeSe are strikingly similar to each other in a wide range of  $t$ . Only below  $t = 0.4$ , the data begin to show the potential of the IBS materials. In contrast, the 122 sample exhibits  $H_{\text{irr}}$  close to that of YBCO at similar  $t$ , which demonstrates the usefulness of the IBS materials operating at low  $T$ .

Overall, for TF magnet applications 3 different material systems are currently available, which all have their advantages and disadvantages. Concerning the highest  $j_c$  values, the REBCO materials show the highest ones, and also exhibit the highest  $H_{\text{irr}}(T)$  of all compounds. Furthermore, REBCO materials enable the use of liquid nitrogen (77 K) as coolant. This advantage is, however, paid for by a specifically devoted and costly preparation technique. The materials with simpler (and cheaper) preparation techniques like  $\text{MgB}_2$  and IBS require the use of cryocooling systems due to their lower  $T_c$ .  $\text{MgB}_2$  to date cannot operate at fields higher than 4 T, even at low temperatures and suffers from the flux jump problem, leading to a chosen operation temperature at 20 K, which is a good compromise. The IBS materials offer high enough currents at high fields and low  $T$ , so they are a good alternative to  $\text{MgB}_2$  without the flux jump problem. Both systems still require further development of the flux pinning properties.

#### IV. CONCLUSION

In summary, we have presented  $j_c(T)$ -data from a variety of samples which are interesting for applications as TF magnets. Plotting  $j_c$  as function of  $t = T/T_c$  enables a direct comparison of the different materials and various preparation routes employed. For TF magnets, the REBCO materials set the goal for the other systems, as both  $j_c(T)$  and  $H_{\text{irr}}(T)$  are the largest ones, being well developed already at  $t = 0.9$ . The  $\text{MgB}_2$  materials suffer from the relatively low  $H_{\text{irr}}(T)$ , but when cooled to low temperatures below 20 K, current densities similar to that of REBCO at 60 K can be reached, provided that additional flux pinning sites are added to the compound (e.g., by C addition). If only trapped fields of about 1-2 T are demanded, then  $\text{MgB}_2$  has the clear advantage of the cheap preparation technology. Finally, IBS materials can also be processed using simple technology, and have the potential for high trapped fields free of flux jumps operating at 4.2 K.

#### ACKNOWLEDGMENT

We would like to thank A. Wiederhold, X. L. Zeng (Saarland University, Germany), C. Chang, T. Hauet (IJL Nancy, France) for assistance during the measurements.

## REFERENCES

- [1] D. C. Larbalestier, A. Gurevich, D. M. Feldmann, and A. Polyanskii, "High- $T_c$  superconducting materials for electric power applications". *Nature*, vol. 414, 2001, pp. 368-377.
- [2] A. Gurevich, "To use or not to use cool superconductors". *Nature Mater.*, vol. 10, 2011, pp. 255 – 259.
- [3] M. Tomita, and M. Murakami, "High-temperature superconductor bulk magnets that can trap magnetic fields of over 17 tesla at 29 K". *Nature*, vol. 421, 2003, pp. 517–520.
- [4] J. H. Durrell, A. R. Dennis, J. Jaroszynski, M. D. Ainslie, K. G. B. Palmer, Y. Shi, A. M. Campbell, J. Hull, M. Strasik, E. Hellstrom, and D. A. Cardwell, "A Trapped Field of 17.6 T in Melt-Processed, Bulk Gd-Ba-Cu-O Reinforced with Shrink-Fit Steel". *Supercond. Sci. Technol.*, vol. 27, 2014, Art no. 082001.
- [5] E. S. Reddy, and G. J. Schmitz, "Ceramic foams". *Am Ceram. Soc. Bull.*, vol. 81, 2002, pp. 3537.
- [6] M. Muralidhar, K. Inoue, M. R. Koblishka, M. Tomita, and M. Murakami, "Optimization of processing conditions towards high trapped fields in MgB<sub>2</sub> bulks". *J. Alloys Compounds*, vol. 608, 2014, pp. 102109.
- [7] J. G. Noudem, M. Aburras, P. Berstein, X. Chaud, M. Muralidhar, and M. Murakami, "Development in processing of MgB<sub>2</sub> cryo-magnet superconductors". *J. Appl. Phys.*, vol. 116, 2014, Art. no. 163916.
- [8] J. D. Weiss, J. Jiang, A. A. Polyanskii, and E. E. Hellstrom, "Mechanochemical synthesis of pnictide compounds and superconducting Ba<sub>0.6</sub>K<sub>0.4</sub>Fe<sub>2</sub>As<sub>2</sub> bulks with high critical current density". *Supercond. Sci. Technol.*, vol. 26, 2013, Art. no. 074003.
- [9] J. D. Weiss, A. Yamamoto, A. A. Polyanskii, R. B. Richardson, D. C. Larbalestier, and E. E. Hellstrom, "Demonstration of an iron-pnictide bulk superconducting magnet capable of trapping over 1 T". *Supercond. Sci. Technol.*, vol. 28, 2015, Art. no. 112001.
- [10] E. Nazarova, K. Buchkov, S. Terzieva, K. Nenkov, A. Zahariev, D. Kovacheva, N. Balchev, and G. Fuchs, "The Effect of Ag Addition on the Superconducting Properties of FeSe<sub>0.94</sub>". *J. Supercond. Nov. Magn.*, vol. 28, 2015, pp. 11351138.
- [11] M. Muralidhar, K. Furutani, D. Kumar, M. R. Koblishka, M. S. Ramachandra Rao, and M. Murakami, "Improved critical current densities in bulk FeSe superconductor using ball milled powders and high temperature sintering". *Phys. Status Solidi A*, vol. 213, 2016, pp. 3214 – 3220.
- [12] T. Katase, Y. Ishimaru, A. Tsukamoto, H. Hiramatsu, T. Kamiya, K. Tanabe, and H. Hosono, "Advantageous grain boundaries in iron pnictide superconductors". *Nature Comm.*, vol. 2, 2011, Art. no. 409.
- [13] K. Iida, J. Hänisch, and C. Tarantini, "Fe-based superconducting thin films on metallic substrates: Growth, characteristics, and relevant properties". *Appl. Phys. Rev.*, vol. 5, 2018, 031304.
- [14] J. Hecher, T. Baumgartner, J. D. Weiss, C. Tarantini, A. Yamamoto, J. Jiang, E. E. Hellstrom, D. C. Larbalestier, and M. Eisterer, "Small grains: a key to high-field applications of granular Ba-122 superconductors?". *Supercond. Sci. Technol.*, vol. 29, 2016, Art. no. 025004.
- [15] K. Nakazato, M. Muralidhar, N. Koshizuka, K. Inoue, and M. Murakami, "Effect of growth temperature on superconducting properties of YBCO bulk superconductors grown by seeded infiltration". *Physica C*, vol. 504, 2014, pp. 4 – 7.
- [16] K. Iida, N. H. Babu, Y. Shi, and D. A. Cardwell, "Seeded infiltration and growth of large, single domain Y-Ba-Cu-O bulk superconductors with very high critical current densities". *Supercond. Sci. Technol.*, vol. 18, 2005, pp. 1421-1427.
- [17] N. D. Kumar, T. Rajasekharan, K. Muralidharan, A. Banerjee, and V. Seshubai, "Unprecedented current density to high fields in YBa<sub>2</sub>Cu<sub>3</sub>O<sub>7δ</sub> superconductor through nano-defects generated by preform optimization in infiltration growth process", *Supercond. Sci. Technol.*, vol. 23, 2010, Art. no. 105020.
- [18] A. Koblishka-Veneva, M. R. Koblishka, N. Ide, K. Inoue, M. Muralidhar, T. Hauet, and M. Murakami, "Microstructural and magnetic analysis of a superconducting foam and comparison with IG-processed bulk samples". *J. Phys. Conf. Ser.*, vol. 695, 2016, Art. no. 012002.
- [19] M. R. Koblishka, A. Koblishka-Veneva, C. Chang, T. Hauet, E. S. Reddy, and G. J. Schmitz, "Flux pinning analysis of superconducting YBCO foam struts". *IEEE Trans. Appl. Supercond.*, DOI: 10.1109/TASC.2018.2880334.
- [20] M. Muralidhar, M. Jirsa, and M. Tomita, "Flux pinning and superconducting properties of melt-textured NEG-123 superconductor with TiO<sub>2</sub> addition". *Physica C*, vol. 470, 2010, pp. 592 – 597.
- [21] M. R. Koblishka, and M. Muralidhar, "Pinning force scaling and its analysis in the LRE-123 ternary compounds". *Physica C*, vol. 496, 2014, pp. 23 – 27.
- [22] K. Berger, M. R. Koblishka, B. Douine, J. Noudem, P. Bernstein, T. Hauet, and J. Leveque, "High magnetic field generated by bulk MgB<sub>2</sub> prepared by spark plasma sintering". *IEEE Trans. Appl. Supercond.*, vol. 26, 2016, Art. no. 6801005.
- [23] M. Muralidhar, M. Higuchi, M. Jirsa, P. Diko, I. Kokal, and M. Murakami, "Improved Critical Current Densities of Bulk MgB<sub>2</sub> Using Carbon-Coated Amorphous Boron". *IEEE Trans. Appl. Supercond.*, vol. 27, 2017, Art. no. 6201104.
- [24] M. R. Koblishka, A. Koblishka-Veneva, M. Muralidhar, and M. Murakami, "Magnetic characterization of bulk C-added MgB<sub>2</sub>". *IEEE Trans. Appl. Supercond.*, vol. 29, 2019, Art. no. 6800104.
- [25] T. Karwoth, K. Furutani, M. R. Koblishka, X. L. Zeng, A. Wiederhold, M. Muralidhar, M. Murakami, and U. Hartmann, "Electrotransport and magnetic measurements on bulk FeSe superconductors". *J. Phys. Conf. Ser.*, vol. 1054, 2018, Art. no. 012018.
- [26] D. X. Chen, and R. B. Goldfarb, "Kim model for the magnetization of hard superconductors". *J. Appl. Phys.*, vol. 66, 1989, pp. 2489-2500.
- [27] Y. Sun, S. Pyon, T. Tamegai, R. Kobayashi, T. Watashige, S. Kasahara, Y. Matsuda, T. Shibauchi, and H. Kitamura, "Enhancement of critical current density and mechanism of vortex pinning in H<sup>+</sup>-irradiated FeSe single crystal". *Appl. Phys. Express*, vol. 8, 2015, Art. no. 113102.
- [28] R. G. Mints, and A. L. Rakhmanov, "Critical state stability in type-II superconductors and superconducting-normal-metal composites". *Rev. Mod. Phys.*, vol. 53, no. 3, 2011, pp. 551-592.
- [29] M. R. Koblishka, A. Wiederhold, M. Muralidhar, K. Inoue, T. Hauet, B. Douine, K. Berger, M. Murakami, and U. Hartmann, "Development of MgB<sub>2</sub>-Based Bulk Supermagnets". *IEEE Trans. Magn.*, vol. 50, 2014, Art. no. 9000504.
- [30] A. Wiederhold, M. R. Koblishka, K. Inoue, M. Muralidhar, M. Murakami, and U. Hartmann, "Electric transport measurements on bulk, polycrystalline MgB<sub>2</sub> samples prepared at various reaction temperatures". *J. Phys.: Conf. Ser.*, vol. 695, 2016, Art. no. 012004.
- [31] V. Sandu, "Pinning force scaling and its limitation in intermediate and high-temperature superconductors". *Mod. Phys. Lett. B*, vol. 26, 2012, Art. no. 1230007.